Journal of Molecular Catalysis A: Chemical 324 (2010) 24–30

Contents lists available at ScienceDirect

Journal of Molecular Catalysis A: Chemical

journal homepage: www.elsevier.com/locate/molcata

Computational catalysis

Rhodium(I) mediated arylation of aldehydes with arylboronic acids under base and water free conditions: A computational study☆

Alma Itzel Olivos Suarez, Joost N.H. Reek, Bas de Bruin*

University of Amsterdam, Van't Hoff Institute for Molecular Sciences (HIMS), Homogeneous and Supramolecular Catalysis, Nieuwe Achtergracht 166, 1018 WV Amsterdam, The Netherlands

ARTICLE INFO

Article history:
Available online 10 March 2010

Keywords:
Arylboronic acid
Rhodium
Aldehyde
Arylation
DFT

ABSTRACT

The mechanism for rhodium(I) mediated arylation of aromatic aldehydes by arylboronic acids under base and water free conditions was investigated with DFT methods. The detailed picture resulting from the calculations is that the reaction proceeds via an internal base mechanism, whereby the initially formed alcoholate (obtained by aryl migration to the aldehyde) attacks the electrophilic boron atom of the coordinated arylboronic acid substrate to facilitate the aryl transfer to the metal. Alternative pathways involving B–C oxidative addition or internal proton transfer followed by β-aryl transfer from thus resulting Rh–O–BPh(OH) moieties are kinetically disfavored. The rhodium atom does not change its oxidation state throughout this whole process, and all steps proceed smoothly within the coordination sphere of rhodium(I). Aldehyde migratory insertion into the Rh^{I}-aryl bond appears to be the rate limiting step ($\Delta G^{\ddagger}$ = +19.4 kcal mol^{-1}) of the catalytic cycle. The subsequent elementary steps involved in the transmetallation process proceed with lower barriers (<+16.3 kcal mol^{-1}). The *cis*-[Rh(OCHPh$_2$)(OBOHPh)(PNH$_2$(OH)$_2$)$_2$] species **R.S.** should be the resting state species under the catalytic conditions according to the DFT calculations.

1. Introduction

Aryl transfer from arylboronic acids to palladium is a key step in among others Susuki–Miyaura cross-coupling reactions [1,2]. These reactions generally require the presence of an external base and water. Formation of anionic borates [B(Ar)(RO)(OH)$_2$]$^-$ under these conditions is thought to facilitate the transfer of the aryl group to the metal. Theoretical calculations on palladium model systems clearly confirmed this hypothesis [3–5].

The addition of arylboronic acids to aromatic aldehydes was first reported by Miyaura employing rhodium(I) catalysts [6,7], and several other interesting rhodium(I) catalysts have been studied since [8–10]. Most of these reactions deal with simple aromatic aldehydes (which are generally easier to arylate than other carbonyl compounds) and non-functionalized phenylboronic acid, but interesting other methods were also developed to achieve arylations of (1,2-di)ketones and (1,2-keto)esters [11–13], imines [14], cyanoformates [15] and α-ketoesters [16], or to use functionalized aldehydes and/or functionalized arylboronic acids [17,18]. Asymmetric versions of these interesting reactions have also been developed based on chiral phosphoramidites [19], phosphites [16] and chiral diene ligands [20,21]. Chiral Rh^{I}(diene) complexes have also been applied in Rh-mediated enantioselective aryl transfer from arylboronic acids to α,β-unsaturated carbonyl compounds and imines [22]. The field is clearly dominated by rhodium(I) catalysis, although some recent reports focused on replacing rhodium by other (cheaper) transition metals such as ruthenium(II) [23], nickel [24], copper [25] and iron [26].

For most of the above reactions (aqueous) basic conditions are generally required/applied, presumably to promote aryl transfer from [B(Ar)(OH)$_2$] via [(RO)(OH)$_2$B]$^-$ to the metal, as is the case in the palladium mediated Susuki–Miyaura cross-couplings. Experimental studies have shown that rhodium-hydroxo intermediates are important in the transmetallation steps of 1,4-addition of organoboronic acids to α,β-unsaturated carbonyl compounds [27], but the exact role of the base in the transmetallation steps of the rhodium(I) mediated systems remains somewhat elusive. To the best of our knowledge, there are no systematic computational studies available to explain the exact role or function of the base (and water) in the transmetallation steps of the rhodium(I) mediated systems. In this perspective, one of the experimental studies by Feringa, de Vries and Minnaard dealing with phosphoramidite rhodium(I) mediated (enantioselective) arylation of aldehydes is therefore particularly interesting, because this system does not strictly require the presence of an external base (nor water) for catalytic activity [19]. The main product obtained by aldehyde arylation is actually [Ar*R*CO–(B(OH)$_2$)]$^-$, which transforms into the

☆ This paper is part of a special issue on Computational Catalysis.

* Corresponding author.
E-mail address: B.deBruin@uva.nl (B. de Bruin).

1381-1169/$ – see front matter © 2010 Elsevier B.V. All rights reserved.
doi:10.1016/j.molcata.2010.03.002

final alcohol products Ar*R*COH only after aqueous workup [19]. The general mechanism for these reactions, as proposed by Feringa, de Vries and Minnaard, is shown in Scheme 1.

As shown in Scheme 1, the rhodium-alcoholate intermediate (obtained by aldehyde insertion into the Rh-aryl bond) is proposed to be responsible for the direct aryl transfer from arylboronic acid to rhodium with liberation of $[ArRCO{-}(B(OH)_2)]^-$. The basic mechanism in Scheme 1 does not give any insight into the proposed transmetallation process, and considering the importance of the reaction a detailed understanding of all elementary steps contributing to the mechanism is required to facilitate future developments by rational strategies. This triggered us to investigate the reaction mechanism of the rhodium mediated arylation of aldehydes in detail using DFT methods. Apart from an interest in the overall reaction mechanism, we were primarily interested in the question why no external base or water is required in the phosphoramidite based rhodium(I) mediated reactions. Since oxidative addition reactions are generally easier for rhodium(I) than for palladium(II), could B–C

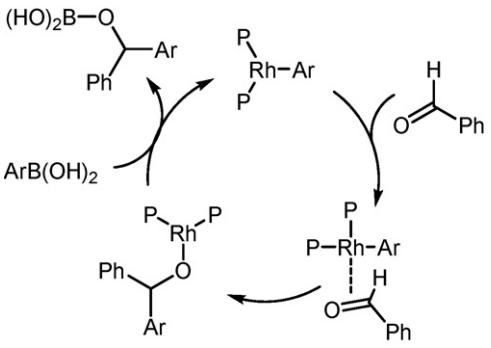

Scheme 1. Proposed mechanism for phosphoramidite rhodium(I) mediated arylation of aldehydes.

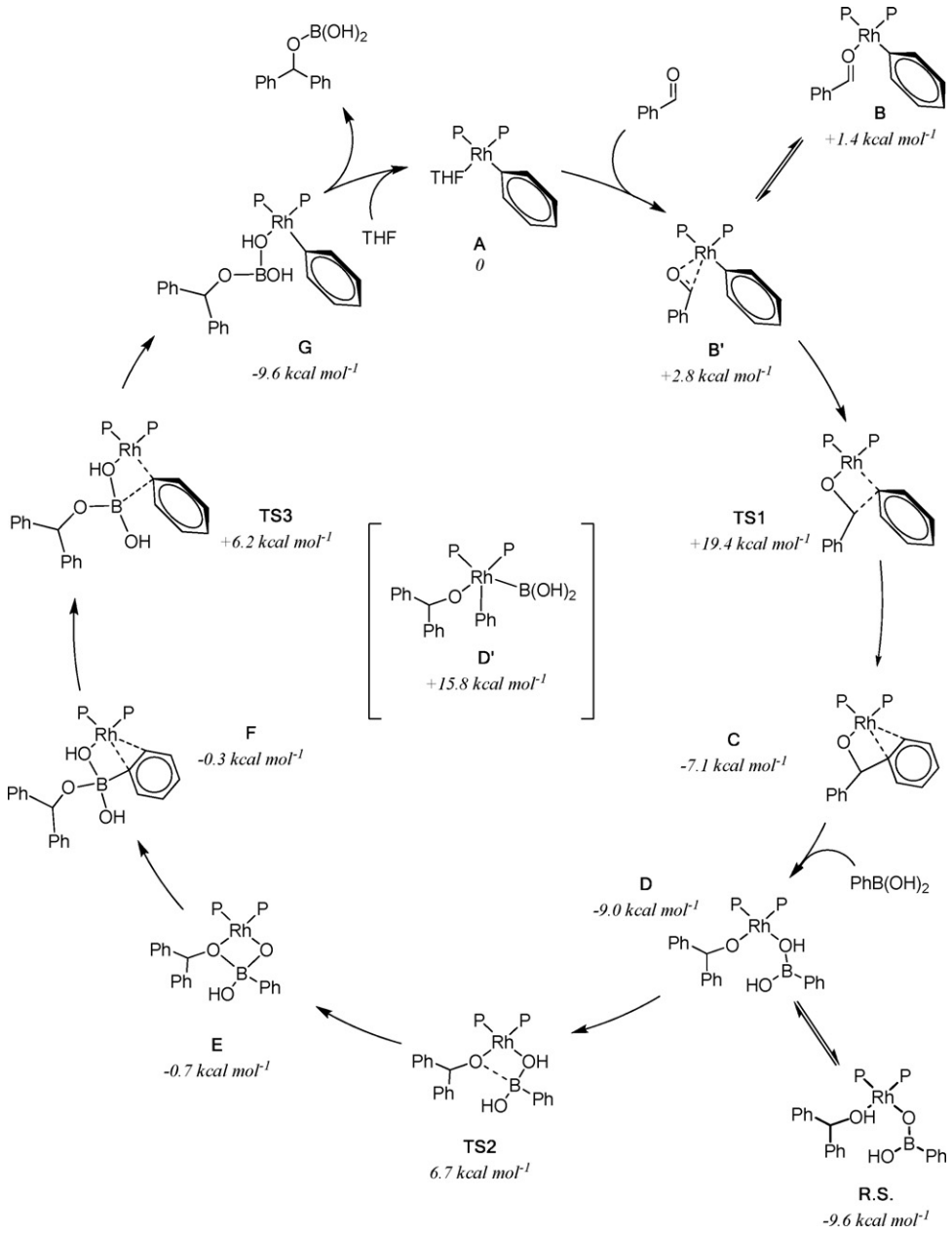

Scheme 2. Summary of the DFT calculated reaction pathways for Rh-mediated arylation of aldehydes with aryl boronic acids (free energies $\Delta G^{\circ}_{298\,K}$, in kcal mol^{-1}, included).

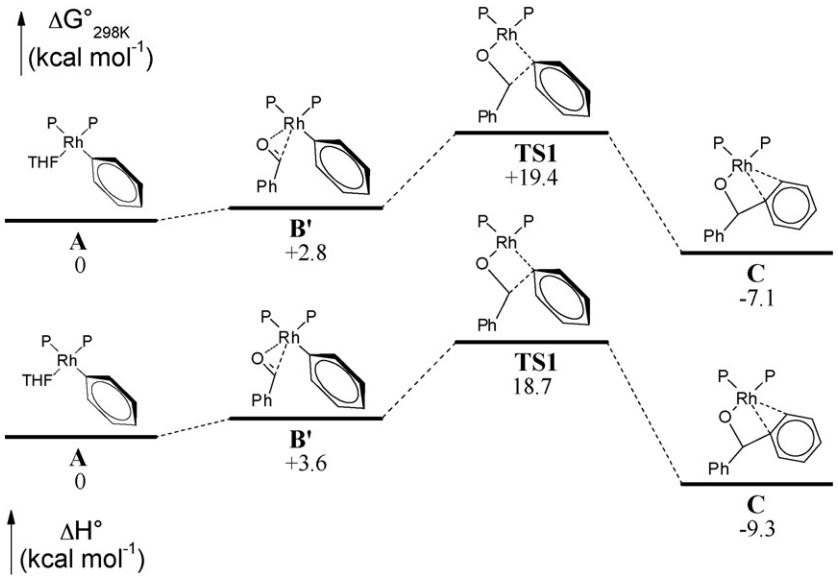

Fig. 1. Free energy ($\Delta G^{\circ}_{298\,K}$; top) and enthalpy ($\Delta H^{\circ}$; bottom) profiles for the formation of alcoholate intermediate **C** from **A**. The free energy (+1.4 kcal mol^{-1}) and enthalpy (+2.0 kcal mol^{-1}) of **B** are not included in the figure for clarity.

oxidative addition play a role in these reactions? . . .or is an internal acid–base reaction within the coordination sphere of rhodium without a change in the oxidation state of the metal a more likely pathway?

2. Results and discussion

The main goal of the DFT investigations in this paper is to provide a detailed picture of the elementary reaction steps contributing to the overall mechanism behind phosphoramidite rhodium(I) mediated arylation of aldehydes under base and water free conditions. We chose not to focus on the enantioselectivities associated with these reactions, and thus we simplified the experimentally applied large chiral phosphoramidite ligands by the much smaller $P(OH)_2NH_2$ ligands to reduce the computation times. We used the Turbomole program package with the Turbomole b3-lyp functional and TZVP basis set supplied with the program for all geometry optimizations (see Section 3.1 for more details).

The proposed starting point in the arylation mechanism according to Feringa, de Vries and Minnaard is a three coordinate species with an anticipated trigonal geometry (Scheme 1). The actual DFT optimized geometry of 3-coordinate species [Rh(Ph)($PNH_2(OH)_2)_2$] (**A-thf**) is T-shaped (mono-vacant square planar). However, this T-shaped species is quite unlikely to exist in solution. The vacant site will immediately be occupied by solvent coordination in the applied coordinating solvents (thf, dioxane, alcohols, toluene/water) [19]. The phenyl starting species is thus much more likely to exist as a square planar solvent adduct. We therefore used the thf adduct *cis*-[Rh(Ph)($PNH_2(OH)_2)_2$(thf)] (**A**) as a starting and energetic reference point for all subsequent steps.

2.1. Aryl transfer to the aldehyde (aldehyde insertion into the Rh–C bond)

Substitution of the thf solvent molecule in **A** by the aromatic aldehyde substrate leads to the square planar aldehyde adduct *cis*-[Rh(Ph)($PNH_2(OH)_2)_2$(κ^1-*O*-{O=CHPh})] (**B**), which has the aromatic aldehyde substrate σ-*O*-coordinated to the Rh atom through one of its carbonyl lone pairs (see Scheme 2 and Fig. 1).

This species has to rearrange to the carbonyl π-*C*,*O*-coordinated isomer *cis*-[Rh(Ph)($PNH_2(OH)_2)_2$(η^2-*O*,*C*-{O=CHPh})] (**B′**), before the phenyl group can migrate to the carbonyl carbon (*vide infra*). The π-carbonyl species **B′** (+2.8 kcal mol^{-1}) is slightly higher in energy than species **B** (+1.4 kcal mol^{-1}). Neither species **B** nor **B′**

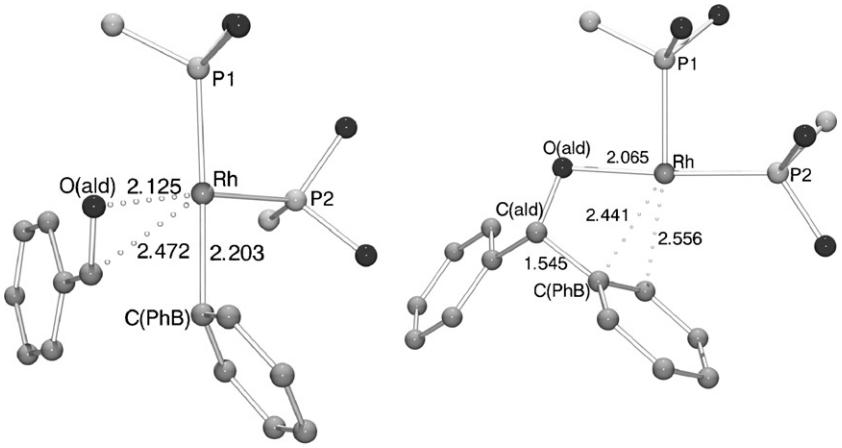

Fig. 2. Geometries of **TS1** (left) and alcoholate intermediate **C** (right).

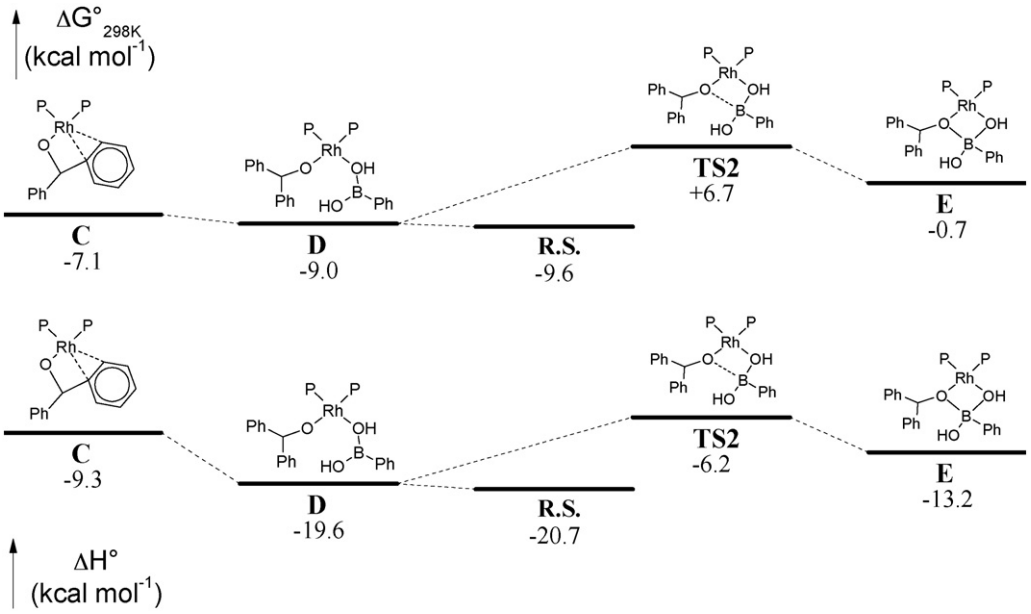

Fig. 3. Free energy ($\Delta G^{\circ}_{298\,K}$; top) and enthalpy ($\Delta H^{\circ}$; bottom) profiles for the formation of borate intermediate **E** from alcoholate **C**.

have affinity for thf at the b3-lyp level of theory, and attempts to optimize the 5-coordinate analogs with DFT led to spontaneous thf dissociation (in both cases).

Phenyl migration to the carbonyl group of **B′** in **TS1** (Fig. 1) has an accessible, though relatively high kinetic free energy barrier (relative free energy of **TS1**: +19.4 kcal mol^{-1}), and this step seems to be rate limiting in the overall catalytic cycle (Scheme 2). This leads to the formation of the alcoholate product *cis*-[Rh(κ^1-*O*-{(OCHPh$_2$)(PNH$_2$(OH)$_2$)$_2$})] (**C**), which is internally stabilized by η^2-aryl coordination of one the two phenyl groups to rhodium (−7.1 kcal mol^{-1}). Remarkably, this pathway resembles the key step of Heck coupling reactions, where an olefinic C=C bond inserts into a Pd–C bond [28] (see Figs. 1 and 2).

The direct migration of the phenyl moiety of **B** to the σ-*O*-coordinated aldehyde moiety was also computationally investigated with a series of constrained geometry optimizations, but this pathway proved to be non-existing. In all attempts, shortening the C_{Ph}–$C_{carbonyl}$ bond along this attempted pathway led to spontaneous formation of (a vibrational exited state of) the π-*C*,*O*-coordinated isomer **B′** before reaching the same transition state **TS1**.

The formation of **C** from **A** is not particularly exergonic, and the DFT calculations thus suggest that these reaction steps should be reversible (see Fig. 1). **C** should be an observable intermediate. The reverse reaction should be kinetically hindered, but in the presence of coordinating agents it should become thermodynamically accessible. These data are in excellent agreement with experimental data from some recently reported model reactions: Hartwig and coworkers reported the spectroscopic and X-ray structural characterization of the alcoholate compound (PEt$_3$)$_2$Rh^{I}–OCPh$_3$, which structurally closely resembles species **C**, including its η^2-aryl coordination mode (Fig. 2) [29]. Heating (PEt$_3$)$_2$Rh^{I}–OCPh$_3$ in the presence of a few additional equivalents of PEt$_3$ leads to β-aryl elimination with formation of the square planar aryl compound (PEt$_3$)$_3$Rh^{I}–Ph and benzophenone (Ph$_2$C=O). Related de-insertion reactions (β-aryl elimination) were synthetically applied in the rhodium(I) catalyzed aryl transfer reactions (1,4-conjugated addition reactions) from trisubstituted aryl alcohols to α,β-unsaturated carbonyl compounds, as reported by the Hayashi group [30–32]. In absence of the electrophilic boronic acid and in the presence of a strongly coordinating medium (e.g. excess of P-ligand) the reverse reaction from **C** leading to β-aryl elimination will indeed become a quite favorable process. Coordination of the boronic acid to form species **D** followed by the subsequent transmetallation steps discussed in the next section should however be the dominant pathway under conditions with an excess of the boronic acid. The presence of other electrophilic species (e.g. protons from water) should also favor the formation of alcohol.

The smooth forward insertion reactions have been unequivocally and directly demonstrated in the case of aldehyde insertions into the Rh–C bonds of square planar Rh^{I}-aryl model compounds [33], and some related insertion and de-insertion reactions of ketones, imines, and nitriles were also elegantly demonstrated by the Hartwig group [32,34,31].

2.2. Transmetallation steps

Under base-free conditions, substitution of the η^2-aryl moiety by a hydroxo moiety of the phenylboronic acid substrate to form *cis*-[Rh^{I}(*O*-CHPh$_2$)(OHBOHPh)(PNH$_2$(OH)$_2$)$_2$] species **D** is perhaps the most logical next step to allow subsequent mechanistic steps for phenyl transfer to the metal (*vide infra*). On the other hand, oxidative addition of the B–C bond of phenylboronic acid to Rh^{I}, thereby forming a Ph–Rh^{III}–B(OH)$_2$ species, could (in principle) be an alternative pathway for formation of [Ar*R*CO–(B(OH)$_2$)]$^-$. The oxidative addition product *cis*-[Rh^{III}(Ph)(B(OH)$_2$)(*O*-CHPh$_2$)(OHBOHPh)(PNH$_2$(OH)$_2$)$_2$] species **D′** is however substantially destabilized ($\Delta\Delta G^{\circ}$ = +15.3 kcal mol^{-1}) compared to **D** (see Figures S1 and S2, Supplementary Material). The kinetic barrier for this process (which we did not consider further) must be even higher in energy, which makes this pathway highly unlikely compared to the transmetallation steps described below.

Indeed, formation of *cis*-[Rh(*O*-CHPh$_2$)(OHBOHPh)(PNH$_2$(OH)$_2$)$_2$] species **D** by substitution of the η^2-aryl moiety in **C** by a hydroxo moiety of the phenylboronic acid substrate is exergonic (ΔG° = −1.9 kcal mol^{-1}, see Fig. 3). From **D**, two transmetallation pathways are conceivable:

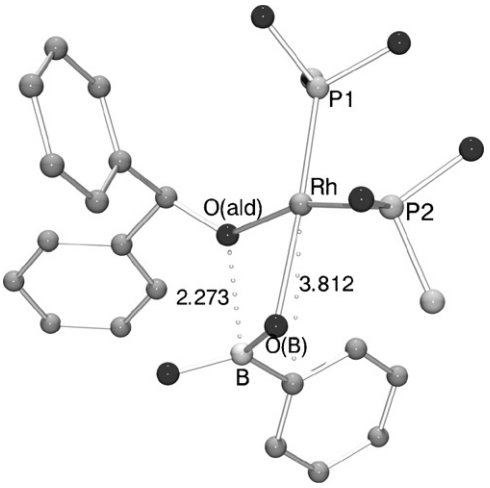

Fig. 4. Geometry of **TS2**.

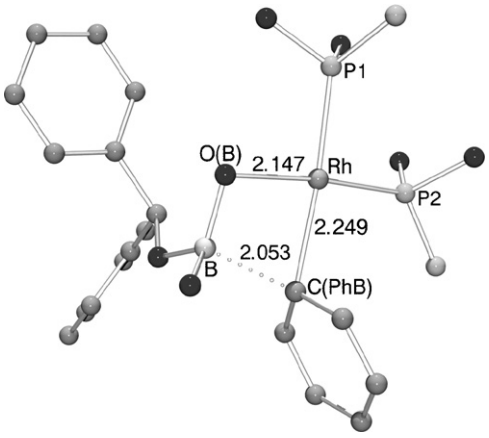

Fig. 6. Geometry of **TS3**.

(I) *Alcoholate migration transmetallation pathway*: Migration of the alcoholate moiety to the electrophilic boron moiety of **D**, followed by phenyl migration from the resulting coordinated anionic hypervalent borate moiety.
(II) *Proton transfer transmetallation pathway*: Protonation of the alcoholate by coordinated boronic acid moiety of **D** to form species **R.S.**, followed by β-aryl elimination from the resulting Rh–*O*–BPh(OH) moiety (trivalent boron) of species **R.S.**

Although the first pathway was considered to be most logical, the free energy of **R.S.** species *cis*-[Rh(OCHPh$_2$)(OBOHPh)(PNH$_2$(OH)$_2$)$_2$] is slightly lower than that of **D** (see Fig. 3) [35], and hence both pathways were considered computationally.

2.2.1. Alcoholate migration transmetallation pathway (I)

Migration of the alcoholate moiety to the borane moiety of **D** via **TS2** (+6.7 kcal mol^{-1}) is a lower barrier process ($\Delta G^{\ddagger}$ = +15.7 kcal mol^{-1}) than the preceding aldehyde insertion steps, and produces the *cis*-[Rh(k^2-*O*,*O*-{(B(OCHPh$_2$)(OH)$_2$(Ph)})(PNH$_2$(OH)$_2$)$_2$)] species **E**. This whole process occurs without dissociation of the 'alcoholate' *O*-donor in **D**. Formation of **E** (−0.7 kcal mol^{-1}) from **C** (−7.1 kcal mol^{-1}) via **TS2** (+6.7 kcal mol^{-1}) should be reversible (see Figs. 3 and 4).

The lower energy of species **R.S.** as compared to **D** raises the total barrier for the transmetallation pathway for phenyl migration via **TS2** to +16.3 kcal mol^{-1} [35]. Species **R.S.** could well be the resting state species in the overall catalytic cycle, but the energy of species **D** is only 0.6 kcal mol^{-1} higher.

Considering the formation of [Ar*R*CO–(B(OH)$_2$)]$^-$ in the experimental systems, phenyl transfer from the borate moiety in **E** to the metal is the most logical next step in the overall reaction mechanism. This process requires dissociation of the "alcoholate" borate oxygen donor and rearrangement to allow the phenyl unit to come close to the metal. The thus formed species **F** (−0.3 kcal mol^{-1}), having a η^2-coordiated phenyl moiety of the borate unit, is only slightly higher in energy than **E** ($\Delta\Delta G^{\circ}$ = +0.4 kcal mol^{-1}) (see Fig. 5).

Phenyl transfer from boron to the metal in **F** via **TS3** (+6.2 kcal mol^{-1}) is a remarkably low barrier process ($\Delta\Delta G^{\circ}$ = +6.5 kcal mol^{-1}), and produces the phenyl species *cis*-[Rh(PNH$_2$(OH)$_2$)$_2$(Ph)(k^1-*O*{(OH)$_2$B(OCHPh$_2$)})] (**G**), having the final borane product (OH)$_2$B(OCHPh$_2$) still coordinated to rhodium (−9.6 kcal mol^{-1}), see also Fig. 6. Substitution of this product by thf completes the catalytic cycle, which is calculated to

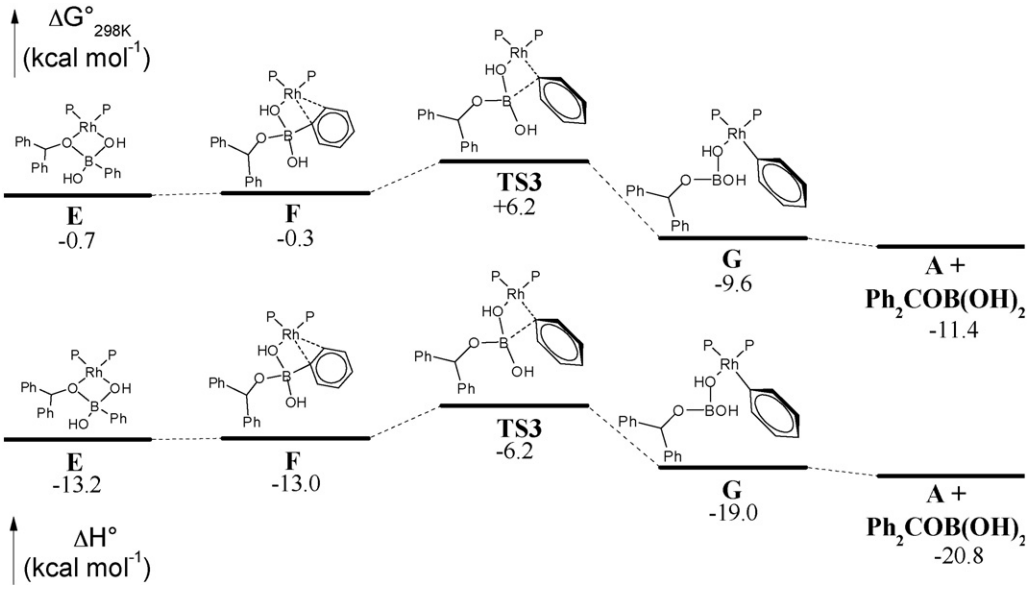

Fig. 5. Free energy ($\Delta G^{\circ}_{298\,K}$; top) and enthalpy ($\Delta H^{\circ}$; bottom) profiles for transmetallation pathway (I) from **E** via **TS3** to regenerate **A**.

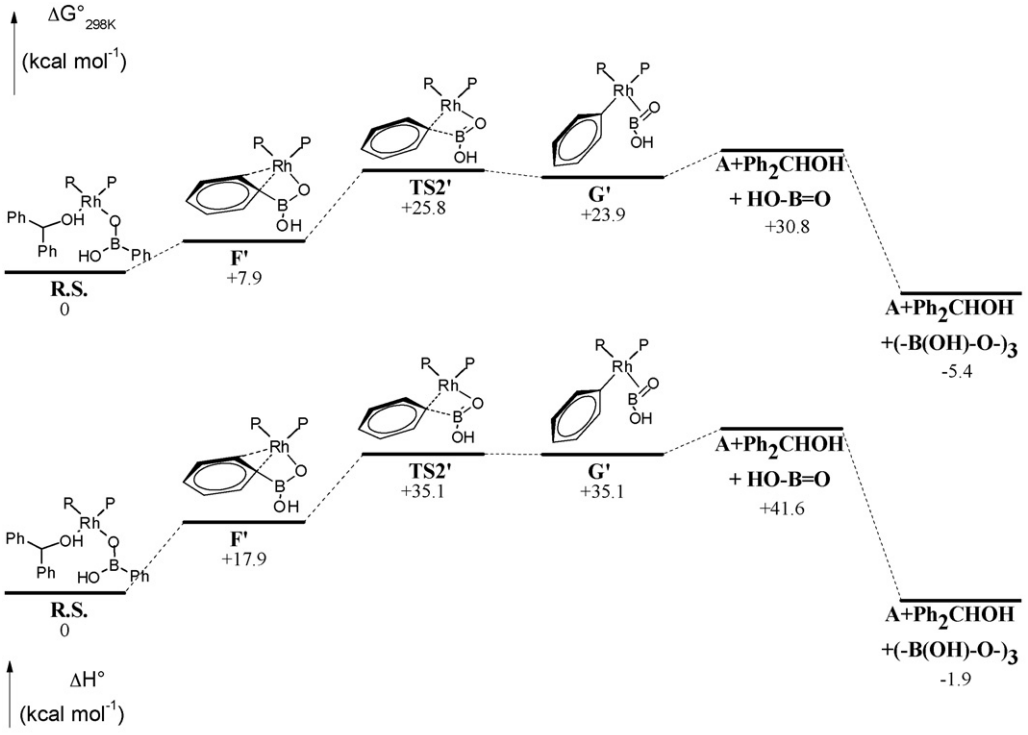

Fig. 7. Free energy ($\Delta G^{\circ}_{298\,K}$; top) and enthalpy ($\Delta H^{\circ}$; bottom) profiles for alternative transmetallation pathway (II) from **R.S.** via **TS2′** to regenerate **A**.

be overall exergonic by −11.4 kcal mol^{-1}. This alcoholate migration transmetallation pathway (I) clearly proceeds with much lower energetic barriers than the oxidative addition process, and conveniently explains the experimentally observed formation of [Ar*R*CO–(B(OH)$_2$)]$^-$.

2.2.2. Proton transfer transmetallation pathway (II)

The relatively low free energy of *cis*-[Rh(OH-CHPh$_2$)(OBOHPh)(PNH$_2$(OH)$_2$)$_2$] species **R.S.** as compared to **D** and **C** potentially allows for an alternative transmetallation pathway involving alcohol dissociation from **R.S.** to form species **F′**, followed by β-aryl elimination (**TS2′**) to produce the Rh^{I}-phenyl species **G′** bearing a π-coordinated HO–B═O moiety. Dissociation of the latter to regenerate **A** is overall endergonic (+30.8 kcal mol^{-1}), but combined with subsequent trimerisation of HO–B═O to (–B(OH)–*O*–)$_3$ the overall process is exergonic by −5.4 kcal mol^{-1} according to the DFT calculations. The overall barrier for this transmetallation pathway, i.e. pathway (II), are substantially higher than those found in the previous section involving alcoholate migration to the coordinated electrophilic boronic acid moiety, i.e. pathway (I). Hence, the sequence in Fig. 7 provides at best an alternative parallel transmetallation pathway, but this reaction channel should play only a minor role in the overall catalytic cycle under base and water free conditions.

Nonetheless, Hartwig and coworkers demonstrated experimentally that the Rh^{I}-amido complex [Rh{N(SiMe$_3$)$_2$}(PEt$_3$)$_2$] reacts with ArB(OH)$_2$ in the presence of excess PEt$_3$ to form [Rh{*O*-BAr(OH)}(PEt$_3$)$_3$] species containing an aryl boroninate ligand (deprotonated aryl boronic acid). These Rh^{I}-OBAr(OH) species undergo β-aryl elimination to produce [Rh(Ar)(PEt$_3$)$_3$] and boroxin oligomers {–*O*–B(OH)}$_n$. Indeed, with the stronger base {N(SiMe$_3$)$_2$} and in the presence of excess PEt$_3$, the formation of the deprotonated aryl boronic acid ligands should be favored, and the pathway from **F′** to **G′** via **TS2′** shown in Fig. 7 basically confirms the proposed β-aryl elimination mechanism by Hartwig for their systems. The obtained barriers according to the DFT calculations appear to be a bit high considering the relatively fast β-aryl elimination reactions observed in the experimental systems, but this may well be related to the electronic influence of the different P-ligands (i.e. strongly σ-donating PEt$_3$ ligands in the experimental systems versus the π-accepting phosphoramidite model PNH$_2$(OH)$_2$ in the DFT calculations).

In any case, the proton transfer transmetalation pathway (II) shown in Fig. 7 should play only a minor role in the mechanism of aldehyde arylation under base and water free conditions, which according to the DFT calculations should be dominated by the alcoholate transmetallation pathway (I) shown in Figs. 3 and 5. Hence, Scheme 2 summarizes the overall computed reaction pathway.

3. Conclusions

We explored the reaction mechanism of rhodium(I) mediated arylation reactions of aldehydes with arylboronic acids, under base and water free conditions, using DFT methods. The detailed picture resulting from the DFT calculations is that the reaction proceeds most likely via an internal base mechanism for the crucial transmetallation steps. Alternative oxidative addition pathways are kinetically disfavored.

The rhodium-alcoholate intermediate (formed by aryl insertion into a Rh-aryl bond) functions as an internal base and attacks the electrophilic coordinated arylboronic acid substrate at boron. The resulting coordinated borate anion subsequently transfers its aryl moiety to rhodium to close the catalytic cycle. The rhodium atom does not change its oxidation state throughout this whole process, and all steps proceed smoothly within the coordination sphere of rhodium. The DFT calculated pathway confirms the mechanism initially proposed by de Vries, Feringa and Minnaard. Somewhat unexpectedly the aldehyde migratory insertion into the Rh-aryl bond is calculated to be the rate limiting step ($\Delta G^{\ddagger}$ = +19.4 kcal mol^{-1}) of the overall catalytic cycle. All subsequent elementary steps involved in the transmetallation process proceed with lower barriers (<+16.3 kcal mol^{-1}).

The *cis*-[Rh(OH-CHPh$_2$)(OBOHPh)(PNH$_2$(OH)$_2$)$_2$] species **R.S.** should be the resting state species under the catalytic conditions according to the DFT calculations, but *cis*-[Rh(*O*-CHPh$_2$)(OHBOHPh)(PNH$_2$(OH)$_2$)$_2$] species **D** is not much higher in energy.

3.1. Applied DFT methods

The DFT geometry optimizations were carried out with the Turbomole program [36a,b] coupled to the PQS Baker optimizer [37]. Geometries were fully optimized as minima or transition states at the b3-lyp level [38] using the polarized triple-ζ TZVP basis [36c,f] (small-core pseudopotential [36c,e] on Rh). All stationary points (minima and transition states) were characterized by vibrational analysis (numerical frequencies); ZPE and gas phase thermal corrections (entropy and enthalpy, 298 K, 1 bar) from these analyses were calculated according to standard formulas of statistical thermodynamics. Estimated condensed phase (1 L mol^{-1}) free energies, entropies and enthalpies were obtained from these data by neglecting the RT term and subsequent correction for the condensed phase reference volume ($S_{\text{condensed phase}} = S_{\text{gas phase}} + R \times \ln(1/24.5)$).

The identity of the transition states was confirmed by following the single negative eigenvalue vibration in both directions (IRC) followed by unconstrained geometry optimizations. Energies are reported in kcal mol^{-1}, both as enthalpies and free energies. The optimized geometries are visualized with the PLATON [39] program (rendered with POVRAY).

Acknowledgements

We thank Dr. Pierre-Alain Breuil for initial discussions. The work was financially supported by the Netherlands Organization for Scientific Research – Chemical Sciences (NWO-CW VIDI project 700.55.426), the European Research Counsel (Grant Agreement 202886) and the University of Amsterdam. We thank a referee for helpful suggestions.

Appendix A. Supplementary data

Supplementary data associated with this article can be found, in the online version, at doi:10.1016/j.molcata.2010.03.002.

References

[1] A. Susuki, Pure Appl. Chem. 66 (1994) 213.
[2] N. Miyaura, A. Susuki, Chem. Rev. 95 (1995) 2457.
[3] A.A.C. Braga, N.H. Morgon, G. Ujaque, A. Lledós, F. Maseras, J. Organomet. Chem. 691 (2006) 4459–4466.
[4] A.A.C. Braga, G. Ujaque, F. Maseras, Organometallics 25 (2006) 3647–3658.
[5] A.A.C. Braga, N.H. Morgon, G. Ujaque, A. Lledós, F. Maseras, J. Am. Chem. Soc. 127 (2005) 9298–9307.
[6] M. Saikai, M. Ueda, N. Miyaura, Angew. Chem. Int. Ed. 37 (1998) 3279.
[7] M. Ueda, N. Miyaura, J. Org. Chem. 65 (2000) 4450.
[8] A. Fürstner, H. Krause, Adv. Synth. Catal. 343 (2001) 343.
[9] S. Uk Son, S. Bok Kim, J.A. Reingold, G.B. Carpenter, D.A. Sweigart, J. Am. Chem. Soc. 127 (2005) 12238–12239.
[10] G. Mora, S. Darses, J.P. Genet, Adv. Synth. Catal. 349 (2007) 1180–1184.
[11] P.Y. Toullec, R.B.C. Jagt, J.G. de Vries, B.L. Feringa, A.J. Minnaard, Org. Lett. 8 (13) (2006) 2715–2718.
[12] S.L.X. Martina, R.B.C. Jagt, J.G. de Vries, B.L. Feringa, A.J. Minnaard, Chem. Commun. (2006) 4093–4095.
[13] G.R. Ganci, J.D. Chisholm, Tetrahedron Lett. 48 (2007) 8266–8269.
[14] R.B.C. Jagt, P.Y. Toullec, D. Geerdink, J.G. de Vries, B.L. Feringa, A.J. Minnaard, Angew. Chem. Int. Ed. 45 (2006) 2789–2791.
[15] H. Shimizu, M. Murakami, Chem. Commun. (2007) 2855–2857.
[16] H.-F. Duan, J.-H. Xie, X.-C. Qiao, L.X. Wang, Q.-L. Zhou, Angew. Chem. Int. Ed. 47 (2008) 4351–4353.
[17] C.-H. Xing, T.-P. Liu, J.R. Zheng, J. Ng, M. Esposito, Q.-S. Hu, Tetrahedron Lett. 50 (2009) 4953–4957.
[18] M. Kuriyama, N. Ishiyama, R. Shimazawa, R. Shirai, O. Onomura, J. Org. Chem. 74 (2009) 9210–9213.
[19] R.B.C. Jagt, P.Y. Toullec, J.G. de Vries, B.L. Feringa, A.J. Minnaard, Org. Biomol. Chem. 4 (2006) 773–775.
[20] T. Nishimura, H. Kumamoto, M. Nagaosa, T. Hayashi, Chem. Commun. (2009) 5713–5715.
[21] T. Noël, K. Vandyck, J. Van der Eycken, Tetrahedron 63 (2007) 12961–12967.
[22] C. Defieber, H. Grützmacher, E.M. Carreira, Angew. Chem. Int. Ed. 47 (2008) 4482–4502 (Review).
[23] Y. Yamamoto, K. Kurihara, N. Miyaura, Angew. Chem. Int. Ed. 48 (2009) 4414–4416.
[24] J. Bouffard, K. Itami, Org. Lett. 11 (2009) 4410–4413.
[25] H. Zheng, Q. Hang, J. Chen, M. Liu, S. Cheng, J. Ding, H. Wu, W. Su, J. Org. Chem. 74 (2009) 934–945.
[26] T. Zou, S.-S. Pi, J.-H. Li, Org. Lett. 11 (2009) 453–456.
[27] T. Hayashi, M. Takahashi, Y. Takaya, M. Ogasawara, J. Am. Chem. Soc. 124 (2002) 5052–5058.
[28] R.F. Heck, P. Nolley Jr., J. Org. Chem. 37 (14) (1972) 2320–2322.
[29] P. Zhao, C.D. Incarvito, J.F. Hartwig, J. Am. Chem. Soc. 128 (2006) 3124–3125.
[30] T. Nishimura, T. Katoh, T. Hayashi, Angew. Chem. Int. Ed. 46 (2007) 4937–4939.
[31] C. Krug, J.F. Hartwig, Organometallics 23 (2004) 4594–4607.
[32] P. Zhao, J.F. Hartwig, Organometallics 27 (2008) 4749–4757.
[33] C. Krug, J.F. Hartwig, J. Am. Chem. Soc. 124 (2002) 1674–1679.
[34] T. Ishiyama, J. Hartwig, J. Am. Chem. Soc 122 (2000) 12043–12044.
[35] We did not consider the barrier for proton transfer in **D** to form species **R.S.**, as this process is most likely solvent assisted. However, such proton transfer reactions are generally low barrier processes, and thus **R.S.** should be easily accessible from **D**.
[36] (a) R. Ahlrichs, M. Bär, H.-P. Baron, R. Bauernschmitt, S. Böcker, M. Ehrig, K. Eichkorn, S. Elliott, F. Furche, F. Haase, M. Häser, C. Hättig, H. Horn, C. Huber, U. Huniar, M. Kattannek, A. Köhn, C. Kölmel, M. Kollwitz, K. May, C. Ochsenfeld, H. Öhm, A. Schäfer, U. Schneider, O. Treutler, K. Tsereteli, B. Unterreiner, M. von Arnim, F. Weigend, P. Weis, H. Weiss, Turbomole Version 5, Theoretical Chemistry Group, University of Karlsruhe, January 2002;
(b) O. Treutler, R. Ahlrichs, J. Chem. Phys. 102 (1995) 346–354;
(c) Turbomole basisset library, Turbomole Version 5, see;
(d) A. Schäfer, H. Horn, R. Ahlrichs, J. Chem. Phys. 97 (1992) 2571–2577;
(e) D. Andrae, U. Haeussermann, M. Dolg, H. Stoll, H. Preuss, Theor. Chim. Acta 77 (1990) 123–141;
(f) A. Schäfer, C. Huber, R. Ahlrichs, J. Chem. Phys. 100 (1994) 5829–5835;
(g) R. Ahlrichs, K. May, Chem. Phys. 2 (2000) 943.
[37] (a) PQS Version 2.4, Parallel Quantum Solutions, Fayetteville, AR, USA, 2001 (the Baker optimizer is available separately from PQS upon request);
(b) J. Baker, J. Comput. Chem. 7 (1986) 385–395.
[38] (a) C. Lee, W. Yang, R.G. Parr, Phys. Rev. B 37 (1988) 785–789;
(b) A.D. Becke, J. Chem. Phys. 98 (1993) 1372–1377;
(c) A.D. Becke, J. Chem. Phys. 98 (1993) 5648–5652;
(d) Calculations were performed using the Turbomole functional "b3-lyp", which is not identical to the Gaussian "B3LYP" functional.
[39] A.L. Spek, PLATON. A Multipurpose Crystallographic Tool, Utrecht University, Utrecht, The Netherlands, 2003.